2012

Vapor Jet Ejector Used To Generate Free Waste Heat Driven Cooling In Military Environmental Cooling Units

Stefan Elbel
stefan.elbel@creativethermalsolutions.com

Chad D. Bowers

Manuel Reichle

Jonathan M. Cristiani

Predrag S. Hrnjak

Vapor Jet Ejector Used to Generate Free Waste Heat Driven Cooling in Military Environmental Cooling Units

S. ELBEL[(1,2,*)], C.D. BOWERS[(1)], M. REICHLE[(1)], J.M. CRISTIANI[(3)], P. HRNJAK [(1,2)]

[1]Creative Thermal Solutions, Inc.
2209 North Willow Road, Urbana, IL 61802, USA
Phone: (217) 344-7663, Fax: (217) 344-7552, Email: stefan.elbel@creativethermalsolutions.com

[2]University of Illinois at Urbana-Champaign
Department of Mechanical Science and Engineering
1206 West Green Street, Urbana, IL 61801, USA

[3]U.S. Army, Communications-Electronics Research Development and Engineering Center (CERDEC)
Command, Power, and Integration Directorate (CP&ID) Power Division 5100 Magazine Road, Aberdeen Proving Ground, MD 21005, USA

* Corresponding Author

ABSTRACT

The waste heat driven vapor jet ejector cooling cycle is a very promising approach to produce 'free' cooling by utilizing low-grade energy sources. The mechanism behind ejector-based waste heat cooling is very different from absorption or adsorption cooling technologies that are also aimed at producing heat driven cooling. The ejector cooling system is actually more closely related to vapor compression technology, in which an ejector, a waste heat source, and a liquid pump are used to replace the vapor compressor. Despite the fact that ejectors were first used in refrigeration systems almost 100 years ago, commercially available waste heat driven ejector cooling systems do not exist at this point. However, this intriguing technology continues to draw significant attention from academia, Government laboratories, and research departments in industry. Rising energy costs and the desire to utilize otherwise unused low-grade energy that becomes available as a byproduct in many processes, such as power generation, justify increased research efforts on this promising approach. This paper presents both numerical and experimental research carried out with vapor jet ejector cooling cycles. A military-style, trailer-mounted technology demonstrator was designed, built, and evaluated. The concept consists of a diesel-electric generator with a nominal electric power output of 15 kW. A conventional, transcritical R744 vapor compression Environmental Control Unit (ECU) is powered by the generator, thereby loading the generator's combustion engine. Waste heat from the generator is extracted at two different temperature levels, namely from the generator's exhaust and engine coolant streams. The extracted heat is transferred to the R134a working fluid inside the vapor jet ejector ECU where it ultimately produces the desired cooling effect. Measurements show that a cooling effect of 1.54 kW can be produced with electrical input of approximately 0.16 kW. It is demonstrated that the total cooling output per liter fuel spent is improved by up to 11 % by operating the ejector system in addition to the conventional vapor compression system.

1. INTRODUCTION

Many industrial processes produce large amounts of excessive heat that is not utilized. The waste heat driven ejector cooling cycle is a very promising approach to utilize low-grade energy for cooling purposes. Much research has been carried out in order to study and improve the vapor jet ejector cooling system (ECS). The main focus of the research conducted are the refrigerants used, the operating conditions, and the characteristic dimensions of the ejector. The main requirements for the working fluid of a vapor jet ejector cooling cycle are its performance as well as its low environmental impact. Roman and Hernandez (2011) compared various refrigerants on their feasibility and performance as a working fluid in an ECS. In their numerical investigation, propane was found to give best results, followed by R134a and R152a. Least favorable working fluids reported in this study are butane and isobutane when compared to the previously mentioned refrigerants. Selvaraju and Mani (2006) experimentally investigated the performance of an ECS with various ejector dimensions at different evaporating, condensing, and generator temperatures. Refrigerant R134a was used and various ejector configurations were evaluated. It was reported that for a given ejector set-up optimum operating conditions exist that result in maximum system performance.

In the present study, the waste heat from a diesel-electric generator is utilized as heat input to the ECS. A prototype demonstrator was designed, built, and evaluated. The refrigerant utilized for this system is HFC R134a. The system was experimentally investigated at different ambient conditions. Furthermore, the characteristic dimensions of the ejector were varied in order to identify an optimum configuration that results in maximum system performance.

2. DESIGN AND INTEGRATION OF THE EJECTOR COOLING SYSTEM

2.1 Preliminary Investigations and Design of Components

Initial investigations were carried out in a breadboard test configuration. Evaporator and condenser panels of the ECS were installed in wind tunnels inside of calorimetric chambers. The waste heat recovery heat exchangers were installed in a diesel-electric generator and connected to the test facility by refrigerant pipes. An adjustable electric air heater was used to simulate various electric loads on the generator. Different system components such as refrigerant pump, expansion device, and heat exchangers were tested in the breadboard test bench prior to integrating them into the trailer-mounted technology demonstrator. Appropriate air flow rates were identified in order to properly size the air moving equipment. Independent measurements were carried out with the diesel-electric generator. The flow rates of the coolant fluid as well the exhaust air stream were determined in order to size and design the waste heat recovery heat exchangers. Also, pressure drop of the coolant as well as on the exhaust side were simulated and measured to reduce any adverse effects on the diesel engine's performance.

2.2 Arrangement and Components of the Waste Heat Recovery Ejector Cooling System

A 3-D CAD drawing of the technology demonstrator is shown Figure 1. The individual subsystems, namely diesel-electric generator, conventional ECU, and ejector ECU are mounted on a military-style flatbed trailer. The components inside the subsystems are interconnected by refrigerant pipes.

Figure 2 schematically illustrates the subsystems of the trailer-mounted technology demonstrator. The subsystems consist of a conventional, transcritical R744 ECU (ECS), an ejector ECU (ECS), and a diesel-electric generator. All components of the vapor compression system (VCS) are located inside a light-weight aluminum housing. The semi-hermetic, piston-type compressor of the VCS has a nominal capacity of 10 kW and a displacement of 26 cm^3. Three air-cooled aluminum microchannel gas cooler panels are utilized to reject heat to ambient air. The gas cooler panels are circuited in parallel on the refrigerant side and operated in a cross-counter-flow configuration. Downstream of the gas cooler panels the refrigerant is routed through the high-pressure side of the aluminum microchannel internal heat exchanger.

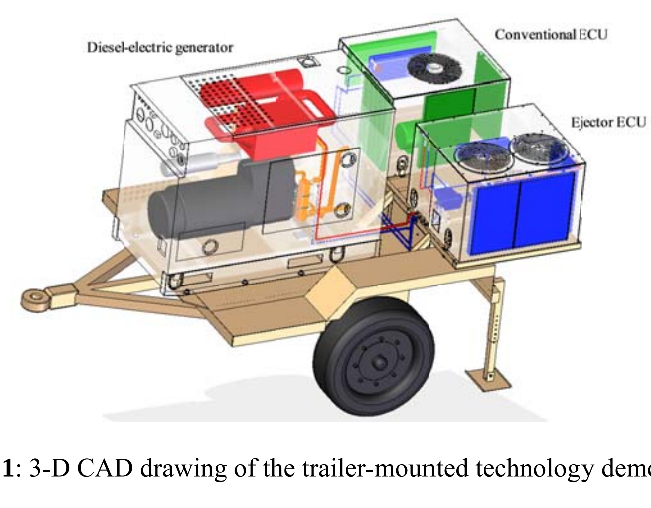

Figure 1: 3-D CAD drawing of the trailer-mounted technology demonstrator

The top-fed aluminum microchannel evaporator has five slabs and is configured in a cross-counterflow arrangement. An electronic expansion valve is utilized to expand the refrigerant into the evaporator where the refrigerant is vaporized, thereby generating a cooling effect. As transcritical R744 systems are typically operated with slightly flooded evaporator, a low-side accumulator with J-tube is installed downstream of the evaporator. The accumulator separates remaining liquid refrigerant from the vapor and serves as a reservoir for excess refrigerant in lower ambient temperature conditions. Refrigerant vapor is drawn from the top of the accumulator along with refrigerant oil from the bottom of the accumulator by a J-tube. Prior to entering the compressor on the suction side, the refrigerant is superheated in the low-pressure side of the internal heat exchanger. The main components of the ECS are installed inside of an aluminum housing similar to the housing of the conventional ECU. A plunger pump is utilized to supply mass flow rate and a pressure increase of the liquid flow. A nitrogen-filled pulsation dampener is installed on the discharge side of the pump in order to eliminate pressure pulsations in the system. Downstream of the pump, the refrigerant is routed to the diesel-electric generator where the waste heat is recovered at two temperatures levels. A brazed-plate copper heat exchanger is arranged in the coolant loop between the diesel engine and the radiator where waste heat is recovered at a lower temperature level. Downstream of the coolant heat exchanger, the refrigerant is routed into the exhaust heat exchanger where waste heat is recovered at a higher temperature level. The exhaust heat exchanger is integrated into the exhaust system of the diesel engine. A diverter valve is used to either route the hot exhaust gas exiting the diesel engine through the exhaust heat exchanger or bypass it when the ejector cycle is not operated. The stainless steel exhaust heat exchanger is of round-tube-and-fin design and operated in a counterflow configuration. The high pressure and high temperature fluid is expanded in the motive nozzle of the ejector, which is designed in a converging-diverging shape. The fluid undergoes significant pressure reduction and acceleration, therefore, the fluid gains kinetic energy that is used to entrain vapor from the evaporator by momentum transfer. Both, motive and suction flows mix inside of the constant area mixing section where the velocities equilibrate and the pressure increases.

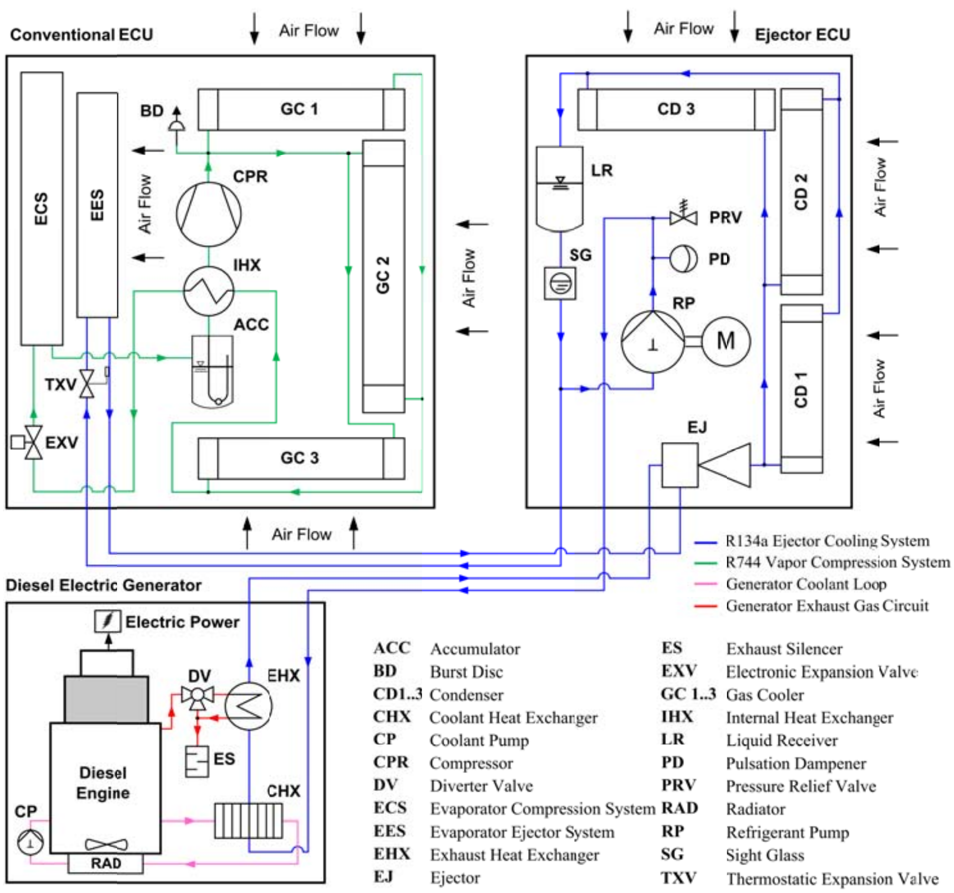

Figure 2: Schematic of the trailer-mounted integrated waste heat recovery ejector system

Possible shock waves can cause a sharp decrease in velocity and a significant pressure rise in the mixing section. In the subsequent diffuser, the remaining kinetic energy is reduced, resulting in a further pressure increase. Downstream of the ejector's diffuser, three air-cooled aluminum microchannel condenser panels are utilized to reject heat to ambient and to liquefy the refrigerant. The condensers are circuited in parallel on the refrigerant-side and configured in a cross-counterflow arrangement. Downstream of the condensers, an accumulator is installed to store excess liquid refrigerant. The refrigerant downstream of the accumulator is split, with the larger amount being fed back to the pump. The remaining portion of the liquid refrigerant is expanded by a thermostatic expansion valve into the aluminum microchannel evaporator. On the air-side, the evaporator of the ECS is installed in series to the evaporator of the VCS. Major benefit of this configuration is the fact that no additional air moving equipment is needed. As the evaporator of the ECS typically operates at higher saturation temperatures, it is located upstream of the evaporator of the VCS. Hence, the air is pre-cooled by the ECS prior to entering the evaporator of the VCS and thus, improving the total cooling output.

Suggestions for ejector dimensions are available in the open literature e.g. ASHRAE (1983) and Selvaraju and Mani (2006). However, an optimum set-up for a particular system still heavily relies on experimental investigations. Therefore, a modular ejector was designed and fabricated as shown in Figure 3a. The ejector components are situated in a steel tube with flanges. Sealing of the individual ejector components is realized by means of PTFE rings. Characteristic dimensions of the ejector are schematically illustrated in Figure 3b. Certain dimensions were kept constant throughout all tests conducted such as throat diameter, length of the motive nozzle diverging and converging section as well as the length of the diffuser. Furthermore, the angles of the motive nozzle divergent section, suction nozzle, and diffuser were kept constant for all tests. Diverging angle of the motive nozzle as well as the mixing section diameter were varied and the effects on the ejector as well as system performance were investigated. Length of the mixing section was adjusted to the corresponding mixing section diameter such that the mixing ratio (l_{ms}/d_{ms}) was maintained at 8.37.

2.3 Experimental Procedure and Instrumentation

Air flow rates across the evaporator and the condenser of the ECS were kept constant. Air inlet temperatures to the evaporator and condensers were adjusted by means of electrical air heaters. Refrigerant superheat at the evaporator exit of the vapor jet ejector cooling system was controlled to be 5 K throughout all tests conducted. The motive mass flow rate was adjusted by varying the speed of the refrigerant pump. As the tests focused on the evaluation of the ECS, the VCS was not operated. Instead, the load on the diesel-electric generator was simulated by using electrical resistance heaters. Electrical output of the diesel-electric generator was kept constant at 10.5 kW, resulting in constant coolant and exhaust temperatures.

Measurements were carried out on the refrigerant-side. Copper-constantan immersion thermocouples (T-type) were used to determine temperatures at the inlet and outlet of each component with an accuracy of ± 0.5 K. Absolute refrigerant pressures were measured by means of piezoelectric pressure transducers with an uncertainty of 0.1 % of the full scale. Pressure drop across heat exchangers was estimated by using piezoelectric differential pressure transducers with an accuracy of 0.25 % of the full scale. Coriolis-effect based mass flow sensors were utilized to quantify the refrigerant mass flow rate of the motive as well as the suction mass flow rate. The manufacturer's lists an accuracy of ± 0.1 % of the full scale for both sensors.

a) 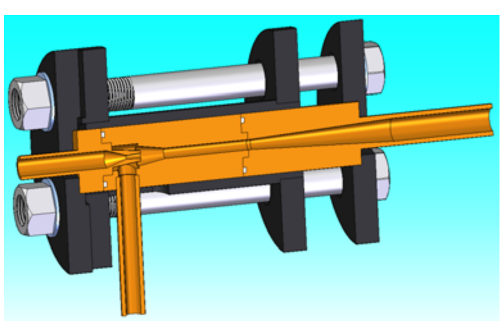

b) 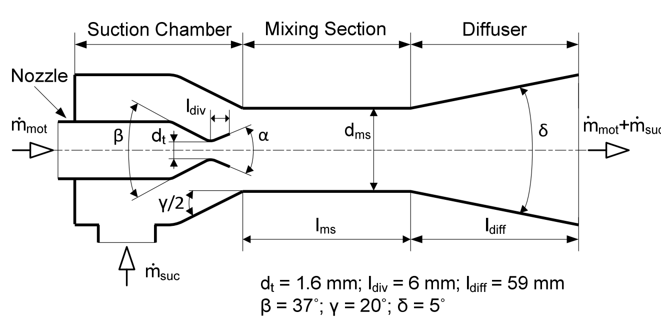

Figure 3: a) 3-D CAD cut-away view of the modular ejector; **b)** schematic of ejector with characteristic dimensions

Power consumption of the refrigerant pump was measured by means of a watt transducer having an accuracy of ± 0.2 % of the full scale. Additionally, thermocouple grids were installed at the inlet and outlet of both evaporators in order to investigate the refrigerant distribution inside the heat exchangers. The instrumentation was calibrated in the range of operation.

3. RESULTS AND DISCUSSION

The performance of the ejector is evaluated using at the mass entrainment ratio and the suction pressure ratio as characterized by Elbel and Hrnjak (2006). The mass entrainment ratio relates the motive mass flow rate to the suction mass flow rate as specified in equation (1). The suction pressure ratio described in equation (2) relates the diffuser exit pressure to the inlet pressure at the suction nozzle.

$$\phi = \frac{\dot{m}_{mot}}{\dot{m}_{suc}} \tag{1}$$

$$\Pi = \frac{p_{diff,out}}{p_{sn,in}} \tag{2}$$

The performance of the ECS can be described by a mechanical COP and a thermal COP (Petrenko et. al., 2011). The mechanical COP (COP_{mech}) compares the cooling output of the ECS to the mechanical work of the pump, whereas the thermal COP (COP_{therm}) relates the cooling output to the amount of waste heat input as described in equations (3) and (4), respectively. It should be noted that the amount of heat added to the system by the pump is neglected in the thermal COP.

$$COP_{mech} = \frac{\dot{Q}_{cool}}{\dot{W}_P} \tag{3}$$

$$COP_{therm} = \frac{\dot{Q}_{cool}}{\dot{Q}_G} \tag{4}$$

The motive nozzle of the ejector has a convergent–divergent shape. According to ASHRAE (1983), values of 10˚ to 12˚ for the angle of the diverging section are most common for steam jet refrigeration, but can range from 8˚ to 15˚. In this study, diverging angles of 8˚, 12˚, and 20˚ were investigated. Experimental results of cooling capacity for various ejector motive nozzle diverging angles are shown in Figure 4a. A very similar trend can be observed for all configurations. The lowest cooling capacity is achieved with the lowest motive mass flow rate. Due to the relatively high inlet temperatures and associated lower densities of the motive vapor flow, velocities inside the ejector are higher. Thus, increased pressure losses are encountered, resulting in reduced entrainment of suction flow. An increase in motive mass flow rate results in increased motive pressure, whereas the inlet temperature of the motive flow is reduced and thus, the cooling capacity increases. Highest cooling capacity of 1.54 kW was observed with a diverging angle of 12˚ and a motive mass flow rate of 30 g/s. A diverging angle of 8˚ seems to be too small and results in pressure losses as the expansion of the motive vapor is restricted. A diverging angle of 20˚ results in the lowest cooling capacity.

Very similar trends can be seen in the mass entrainment ratio and suction pressure ratio as presented in Figure 4b. The ejector configuration with 12˚ diverging angle results in mass entrainment ratios of up to 0.32 with a corresponding suction pressure ratio of approximately 1.9. Significantly lower values are achieved with motive nozzle diverging angles of 8˚ and 12˚.

Experimental results for COP_{therm} are presented in Figure 5a. Increased motive mass flow rate results in an increased amount of heat recovered. However, the increase in cooling capacity is greater than the increase in waste heat recovered. Hence, COP_{therm} increases with increasing motive mass flow rate.

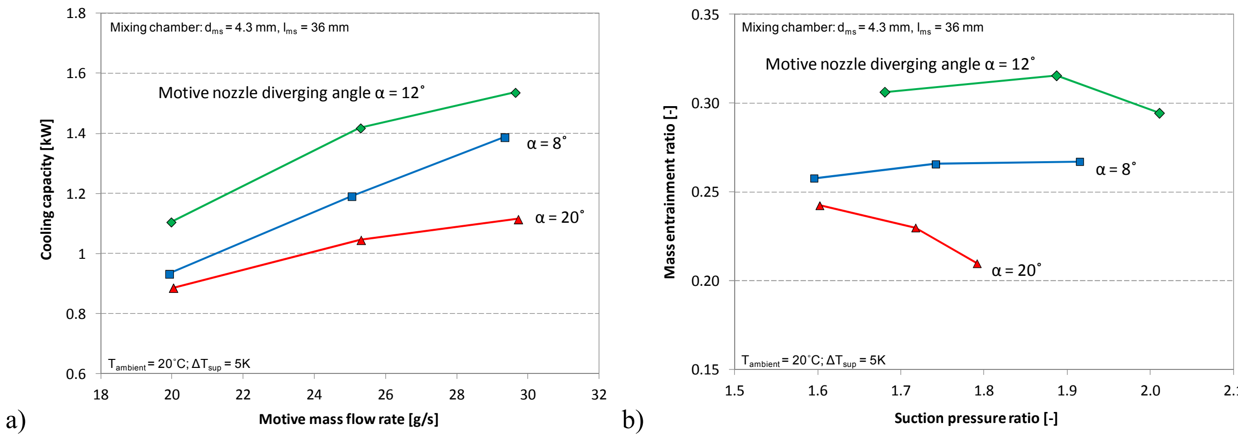

Figure 4: a) Experimental results of cooling capacity for various motive nozzle diverging angles as a function of the motive mass flow rate; **b)** experimental results of mass entrainment ratio for various motive nozzle diverging angles as a function of the suction pressure ratio

The reverse trend can be seen in Figure 5b, where the COP_{mech} decreases with increasing motive mass flow rate. The reason for this is a greater increase in pump power consumption than the increase in cooling capacity. As a result, the highest COP_{mech} of 11.4 is achieved at a condition where the cooling capacity for a given ejector configuration is the lowest.

A variation of mixing chamber diameter d_{ms} with constant ejector throat diameter d_t results in a different ejector area ratio (EAR) [where EAR = d_{ms}^2/d_t^2]. Generally, ejectors with higher EARs yield larger entrainment ratios, whereas smaller EAR values suffer from increased losses caused by friction (Selvaraju and Mani, 2006).

Figure 6a presents results of the cooling capacity for different EARs as a function of the motive mass flow rate. At relatively low motive mass flow rates, the configuration having an EAR of 7.22 shows significantly higher cooling capacity than the one with an EAR of 6.25. In this condition, the motive nozzle inlet temperatures are relatively high, resulting in low densities. Thus, the friction losses in the 4 mm mixing section are higher, which reduces the mass entrainment ratio as shown in Figure 6b. At increased motive mass flow rates the performance of the configuration with EAR 6.25 and 7.22 are very similar. An EAR of 9.77 seems to be too large with no measurable cooling capacity at a motive mass flow rate of 20 g/s. Even at increased motive mass flow rates of 25 g/s and 30 g/s almost no suction flow is entrained which leads to a very low cooling capacity for this configuration.

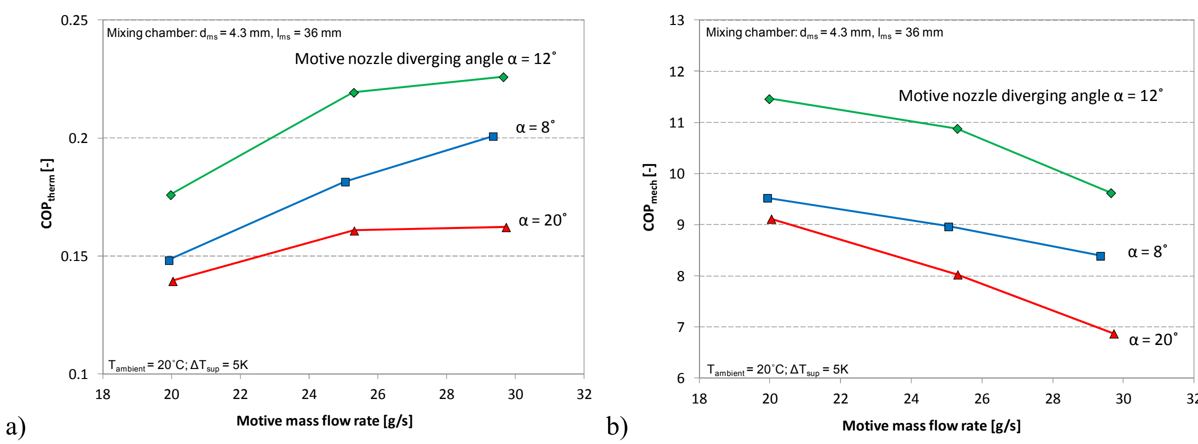

Figure 5: Experimental results of **a)** COP_{therm} and **b)** COP_{mech} for various motive nozzle divergent angles as a function of the motive mass flow rates

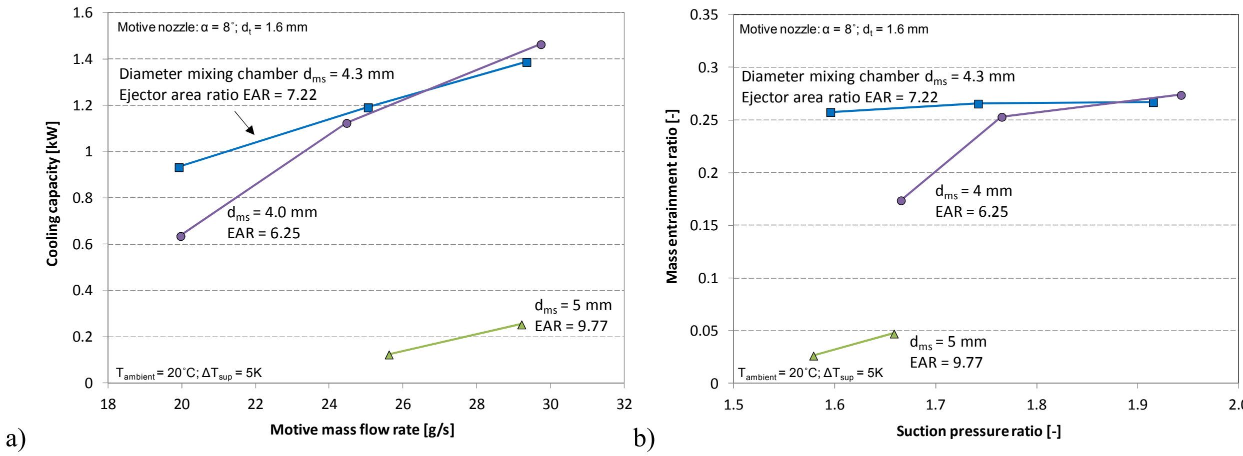

Figure 6: a) Experimental results of cooling capacity for different ejector area ratios as a function of the motive mass flow rate; **b)** experimental results of the mass entrainment ratio for different ejector area ratios as a function of the suction pressure ratio

Results of COP_{therm} and COP_{mech} for different EARs are presented in Figure 7a and Figure 7b, respectively. Trends are very similar to those observed in the corresponding cooling capacity and mass entrainment ratio for a given ejector configuration. A motive mass flow rate of 20 g/s and an EAR of 7.22 yielded the highest COP_{mech}. Values of COP_{therm} and COP_{mech} become almost identical at increased motive mass flow rates, with the smaller EAR of 6.25 having slightly better COP_{therm} and COP_{mech} with a motive mass flow rate of 30 g/s. The EAR of 9.77 results in significantly lower COP values due to a low mass entrainment ratio.

Performance evaluation of the ECS was carried out according to U.S. Army standard test conditions. Conditions D0, D0.5 and D1 denote the air inlet temperatures to both evaporator and condenser of 20 ˚C, 25 ˚C, and 32.2 ˚C, respectively. The performance of the VCS was independently evaluated in an earlier study. However, it should be noted that performance numbers for the conventional system in the conditions D0 and D0.5 are extrapolated, as only experimental performance data for higher ambient temperatures were readily available. As shown in Figure 8a, the cooling capacity of the VCS increases at higher ambient temperature conditions to a maximum of approximately 12 kW at condition D1. The cooling capacity of the ECS decreases with increased ambient temperature. An elevated condenser air inlet temperature increases the condensing pressure. Thus, the driving pressure ratio between generator pressure and condensing pressure is reduced, resulting in less energy available to entrain suction flow from the evaporator. Cooling capacities realized with the ECS ranged from a maximum of 1.54 kW at condition D0 to 0.86 kW at condition D1.

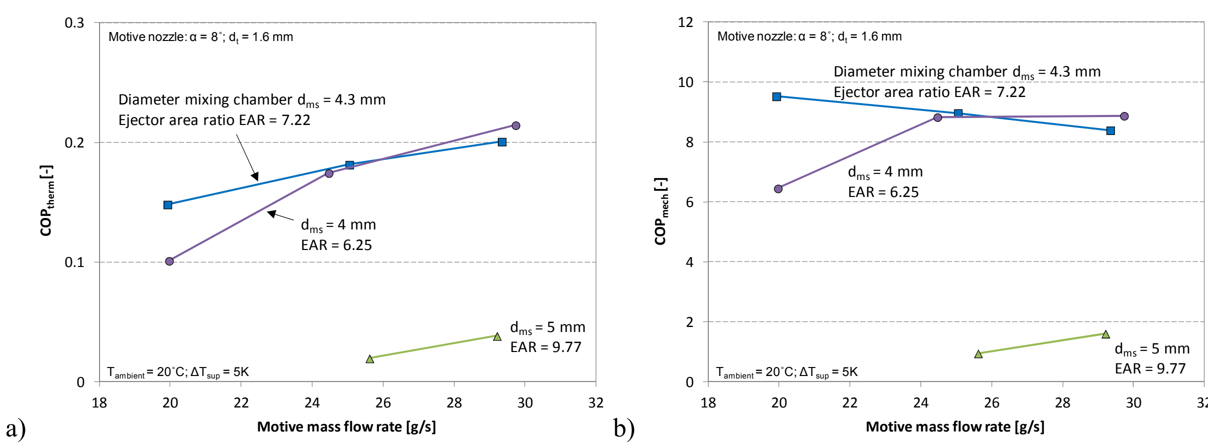

Figure 7: Experimental results of **a)** COP_{therm} and **b)** COP_{mech} for different ejector area ratios as a function of the motive mass flow rat

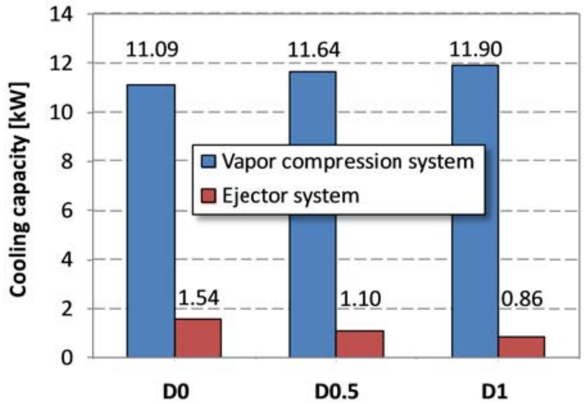

a)

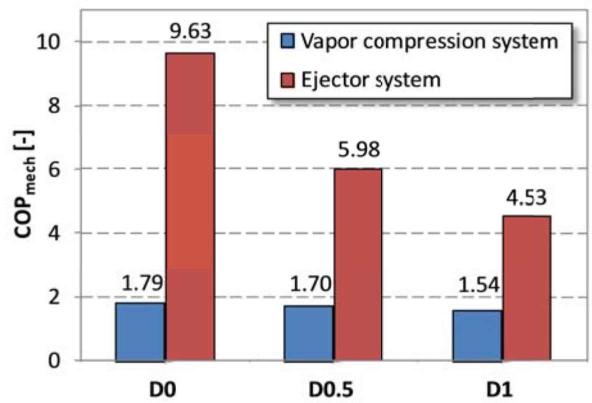

b)

Figure 8: Comparison of **a)** cooling capacity and **b)** COP_{mech} between the conventional and vapor jet ejector system at various ambient temperature conditions

Trends of COP_{mech} are the same for both systems as presented in Figure 8b. Despite an increasing cooling capacity, the COP_{mech} of the VCS decreases as the compressor power consumption increases at higher ambient conditions. Also, COP_{mech} of the ECS is reduced at higher ambient temperature conditions because of the reduced cooling capacity.

In order to demonstrate the overall system improvement by the ECS, the performances of both systems are compared and the efficiency in terms of fuel consumption by the diesel-electric generator calculated. Figure 9 presents the cooling capacity per unit of volumetric fuel consumption for only the VCS operating as well as for both systems operating simultaneously. Numbers are based on a fuel consumption of 0.378 l/kWh$_{el}$, as specified by the manufacturer of the diesel-electric generator (Army, 1992). The total cooling capacity per liter fuel consumed is improved from 4.76 kWh/l to 5.28 kWh/l at condition D0, which corresponds to an improvement of 11%. At higher ambient temperature conditions, the improvement by the ECS decreases due to the reduction in cooling capacity. The calculated improvement at the condition D0.5 is 6.6% and 4.6% at the condition D1, respectively.

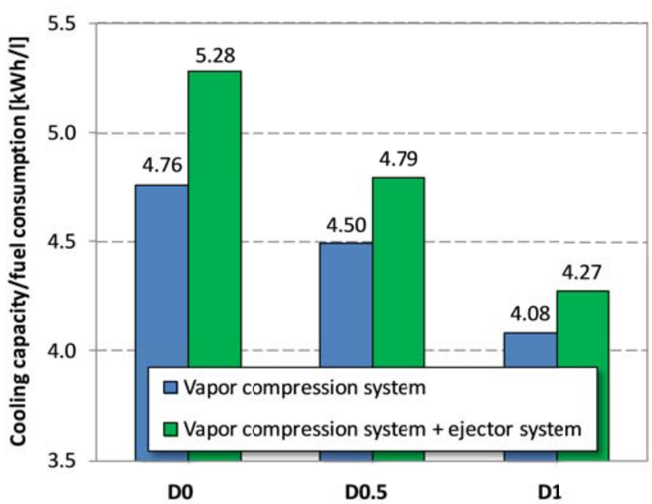

Figure 9: System comparison of cooling output per fuel consumption

4. CONCLUSIONS

In this study, a waste heat driven vapor jet ejector cooling system was designed, built, and experimentally evaluated. Waste heat from a diesel-electric generator was utilized to drive the vapor jet ejector cooling cycle. Characteristic dimensions of the ejector were varied. A motive nozzle converging angle of 12˚ yielded a maximum performance in terms of mass entrainment and cooling capacity. Moreover, a mixing section diameter of 4.3 mm resulted in best results in comparison to a mixing section diameter of 4.0 mm and 5.0 mm. Furthermore, the system performance was evaluated at various ambient temperature conditions. As expected, the system performance decreased at elevated ambient temperatures due to a reduced cooling output. Maximum cooling capacity of 1.54 kW was achieved with an electric input only 0.16 kW, resulting in a COP_{mech} of 9.63. As the cooling output of the ECS was employed to improve the performance of the VCS, fuel consumption of the diesel-electric generator was calculated for only the vapor compression cycle operating in comparison to both systems operating. It was demonstrated that the total cooling output per liter fuel spent can be improved by up to 11%.

NOMENCLATURE

3-D	three dimensional	
CAD	computer aided design	
COP	coefficient of performance	(-)
d	diameter	(mm)
EAR	ejector area ratio	(-)
ECU	environmental control unit	
ECS	ejector cooling system	
HFC	hydrofluorocarbon	
l	length	(mm)
$\dot{m}$	mass flow rate	(kg/s)
p	pressure	(MPa)
PTFE	polytetrafluoroethylene	
$\dot{Q}$	cooling capacity	(kW)
VCS	vapor compression system	
$\dot{W}$	power consumption	(kW)
Subscripts		
cool	cooling	
div	diverging	
diff	diffuser	
el	electric	
G	generator	
in	inlet	
mech	mechanical	
ms	mixing section	
out	outlet	
P	pump	
suc	suction	
sup	superheat	
t	throat	
therm	thermal	
Greek letters		
α	diverging angle	(°)
β	converging angle	(°)
γ	suction nozzle angle	(°)
δ	diffuser angle	(°)
ΔT	temperature difference	(K)
Π	suction pressure ratio	(-)
Φ	mass entrainment ratio	(-)

REFERENCES

American Society of Heating, Refrigerating, and Air-Conditioning Engineers (ASHRAE), 1983, *Handbook: Equipment*, *Chapter 13: Steam-jet refrigeration equipment*, Atlanta, GA

Army, 1992, *Technical Manual MEP-804A TM6115-01-274-7338*, Headquarters Departments of the Army and Air Force, Washington DC

Elbel, S., Hrnjak, P., 2006, Experimental Validation and Design Study of a Transcritical CO2 Prototype Ejector System, *Proc. 7th IIR Gustav Lorentzen Conference on Natural Working Fluids*, Trondheim, May 28 -31, 2006

Petrenko, V., Volovyk, O., Ierin, V., Shestopalov, K., Huang, B.J., 2011, Solar and waste heat driven advanced ejector refrigerating machines operating with low boiling refrigerants, *Proc. Prague,* 23rd IIR International Congress of Refrigeration: Paper ID169

Roman, R., Hernandez, J.I., 2011, Performance of ejector cooling system using low ecological impact refrigerants, *Int. J. Refrig*., vol. 34: p.1707-1716

Selvaraju, A., Mani, A., 2006, Experimental investigation on R134a vapour ejector refrigeration system, *Int. J. Refrig*., vol. 29: p. 1160-1166

ACKNOWLEDGEMENT

The authors gratefully acknowledge the support given by US Army RDECOM. Project funding was made available through ARRA 2009, under contract W909MY-10-C-0001.